Indian Journal of Geo Marine Sciences
Vol. 46 (05), May 2017, pp. 884-892

Light absorption characteristics of chromophoric dissolved organic matter (CDOM) in the coastal waters of northern Bay of Bengal during winter season

Sourav Das[*1], Sugata Hazra[1], Sandip Giri[1], Isha Das[1], Abhra Chanda[1], Anirban Akhand[2] & Sourav Maity[3]

[1]School of Oceanographic Studies, Jadavpur University, 188, Raja S. C. Mullick Road, Kolkata 700 032, West Bengal, India
[2]Coastal and Estuarine Environment Research Group, Port and Airport Research Institute, 3-1-1, Nagase, Yokosuka 239-0826, Japan
[3]Indian National Centre for Ocean Information Services, Hyderabad – 500090, Telengana, India

*[E-mail: sourav.biooptics@gmail.com]

Received 29 July 2015; revised 15 October 2015

Absorption spectra of chromophoric dissolved organic matter (CDOM) and other physico-chemical components were measured in the coastal water of northern Bay of Bengal (nBoB) lying adjacent to West Bengal coast, India, during October, 2014-March, 2015. Absorption coefficient [$a_{CDOM}(440)$] of CDOM exhibited a considerable inverse linear relationship with salinity in the surface waters implying traditional mixing effect of marine and fresh water. A dominant terrestrial CDOM signal influenced by higher fresh water discharge from the river Hugli was seen prior of winter (October, 2014). However, during January, $a_{CDOM}(440)$ value again increased along with a concomitant increase in chlorophyll-*a*. However, total suspended matter (TSM) showed strong linear positive and consistent relationship with $a_{CDOM}(440)$ throughout the study period, ascertaining terrestrial source of CDOM. Moreover, prior of winter, study site receives more discharge from rivers with corresponding signals of lower slope value indicating less aged and high molecular weight of CDOM.

[**Keywords:** Chromophoric dissolved organic matter (CDOM), Absorption, Spectrum, coastal water, northern Bay of Bengal]

Introduction

In shallow continental shelves and estuaries throughout the world, availability of light in the water column is considered to be one of the most crucial factors from the perspective of phytoplankton dynamics along with primary production[1]. The availability of light in the water column is mainly governed by four principal factors namely: the water itself, the phytoplankton abundance and type, the non-living particulate matters and lastly the chromophoric dissolved organic matter (CDOM)[2,3]. Based on the optical characteristics, the natural hydrosphere is generally classified into two groups; Case 1 and Case 2 waters[4]. In Case 1 waters phytoplankton mainly controls the absorption of light (most open ocean and many coastal waters), while in Case 2 waters the non-biogenic particles and CDOM are relatively more important compared to phytoplankton (most estuarine waters fall in this category)[1]. So, because of its influence on aquatic light absorption, CDOM is one of the essential factors of the visible wavelength remote sensing signal collected by satellites. To estimate the chlorophyll concentration from space, quantification and compensation of CDOM is very much necessary[5].

A wide array of compounds like carbohydrates, amino acids, hydrocarbons and phenolic acids have so far been identified as a part of dissolved organic matter (DOM) available in natural waters and many other compounds are yet to be characterized[6,7]. A fraction of this DOM which exhibits strong absorption of short wavelength radiation and imparts a color to the natural water is termed as CDOM[8]. The CDOM concentration is known to vary both spatially and temporally, as it significantly depends upon the variations in freshwater inputs, estuarine mixing process, in-situ primary production and bacterial degradation of phytoplankton[1]. On the other hand, the absorption of light by CDOM in turn regulates many essential near surface processes like heat transfer and several photo-chemical reactions[9,10].

However, the region specific assessment of CDOM

has gained momentum in recent days mainly in order to correctly analyze the chlorophyll-*a* (Chl-*a*) from remotely sensed data. The remote sensing algorithms for assessment of chl-*a*, in the case-II waters, have a tendency to overvalue due to co-absorbing components i.e. CDOM[11]. Hence, appropriate corrections should be made for CDOM and detrital particles in the absorption balance equation:

$a_T = (a_{ph} + a_{CDOM} + a_D)$

where a_{ph}, a_{CDOM} and a_D are absorption coefficients of phytoplankton, CDOM, and detrital particles, respectively, and a_T is total non-water absorption coefficient[12,13,14]. However, in the semi-enclosed coastal seas, the dominant source of CDOM is terrestrial organic debris transported by rivers[15,8,16]. Hence, the correction factors for a_D and a_{CDOM} in remote sensing algorithms for the estimation of chl-*a* in coastal waters has a spatio-temporal variability[17]. In order to address this issue, assessment of CDOM should be downscaled to regional level in order to properly account all the possible criteria that are leading to the overestimation of chl-*a*.

UV-Visible absorption spectra for CDOM increase exponentially with decreasing wavelength[18]. To extort information from these spectra about CDOM properties (qualitative), several spectral parameters, namely; absorption ratio, slope have been defined. These ratios are largely independent of CDOM concentration, which is important in regimes such as mixing zone of ocean and fresh water, where CDOM concentrations often vary by different factors. The intensity of absorption coefficient (a (λ)) at a specific wave length (λ) is used as an expression of the concentration of CDOM (quantitative). The slope of absorption spectrum indicates changes in CDOM composition. The dilution of a concentrated CDOM samples results in a decrease in a (λ) but no significant changes to the shape of the absorption spectrum[19].

The present paper has been conceptualized keeping the importance of region-specific CDOM estimation and characterization, in mind. In this study the CDOM has been assessed as $a_{CDOM}(440)$ and $slope_{(400-700)}$ for the first time in the shallow continental shelf waters lying adjacent to the West Bengal coast in the northern end of the Bay of Bengal. The primary objective of this paper was to examine the variability of $a_{CDOM}(440)$ and its relationship with physico-chemical properties like sea surface salinity (SSS), total suspended matter (TSM) and with chl-*a* concentration during the study period (October 2014 to March 2015) mainly covering the span of winter season and to scrutinize the size and composition of CDOM in terms of slope.

Materials and Methods

Study Area

The present study has been carried out in the northern part of the Bay of Bengal (lying adjacent to the West Bengal coast) (Fig. 1). This region is situated just beside the confluence of the Hugli Estuary and in the north it is bounded by the Indian Sundarban mangrove ecosystem. The Sundarban is the world's largest single stretch of mangrove forest. Due to the presence of mangrove ecosystems in vicinity and an intricate network of creeks and channels, the flushing of tidal ebb through such an ecosystem makes this region rich in organic loading. The study region receives enormous amount of freshwater discharge from the perennial River Hugli that peaks during the monsoon[20, 21] and the consequence also observe in the prior month of winter (October). The Hugli River is a distributary of River Ganges and flows along the western part of Sundarban mangrove ecosystem. This Hugli estuary receives the freshwater flow from the Farakka barrage situated 286 km upstream from the river confluence [22]. There are several other distributaries like (from west to east) the Rivers Muriganga, Saptamukhi, Thakuran, Matla, Gosaba and Bidya which have further added organic matter into study region. The primary production of the study region is also dependent on the availability of solar radiation, which is relatively higher during the winter [23, 24] in the Bay of Bengal.

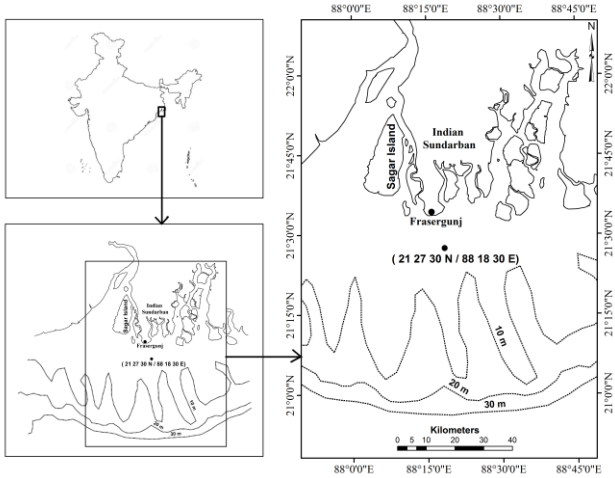

Fig. 1—Study site showing the sampling station

The present survey has been conducted at a station (21º 27' 30" N; 88 º 18' 30" E) ~ 17 km from the shoreline in the shallow continental shelf waters (< 10 m bathymetry) throughout the study period. All the cruises started from Frasargunje Fishing Harbour (Lat. 21º 34' 45.91" N; Long. 88º 15' 5.38"E).

Sampling Strategy

In total twelve (12) sampling surveys were undertaken between October 2014 and March 2015. Two (02) surveys were conducted in each month. Fishing trawlers were hired for each sampling survey. The entire sampling was accomplished in the daytime during high tide. The engine was stopped for 15-20 minutes before collecting each sample, so as to provide the immediate ambience a minimum time to attain the equilibrium. Seawater samples were collected using a 5 L Niskin sampler (General Oceanics, Inc.) from the water surface. Physico-chemical parameters like sea surface temperature (SST), SSS and dissolved oxygen (DO) were analyzed immediately onboard. Samples were transferred into a pre-rinsed container from the Niskin sampler for TSM analysis. For chl-*a* estimation, water samples were filtered through GF/F (Whatman, 47 mm diameter) filter paper on boat and the filter papers were kept in the liquid nitrogen cylinder till analyze in the chemical laboratory. Water samples were filtered using 0.45 µm GF/C (Whatman, 47 mm diameter) filter paper on boat and stored at 4ºC for nutrients analysis in the laboratory within 24 hours.

Analytical Protocol

SSS was measured using a Multikit (WTW Multi 340 i Set; Merck, Germany) fitted with the probe WTW Tetracon 325. pH and SST were measured instantaneously with a micro-pH meter (pH 620; Eutech Instruments, Singapore) having a precision of 0.001 pHu. The glass electrode for pH measurements were calibrated daily in the NBS scale with technical buffers of pH 4.01 (Part no: 1.09475.0500; Merck), pH 7.00 (Part no: 1.09477.0500; Merck) and pH 9.00 (Part no: 1.09476.0500; Merck) at a controlled temperature of 25ºC. The pH readings taken on-board at the respective temperatures were corrected for the standard temperature of 25ºC. Chl-*a*, TSM, Dissolved inorganic nitrate (DIN), dissolved inorganic phosphate (DIP) and reactive silicate (DSi) were analyzed following standard methods and procedures [25].

Nutrient concentrations were expressed in µM. DO was determined using modified Winkler titration[26] employing automated potentiometric detection of endpoint.

CDOM Sampling and Analysis

Seawater samples were collected using a 5 L Niskin sampler (General Oceanics, Inc.) For CDOM, about 100 ml sample were filtered under dim light and gentle vacuum through 0.22 µm Millipore polycarbonate membrane filter, which had been briefly (5 min) soaked in purified water, into precombusted amber colored bottle. All samples are analyzed within 6 hrs of sampling.

Absorbance measurements of CDOM were made in a Shimadzu UV-Visible 1600 double-beam spectrophotometer in the laboratory in 10 cm path length quartz glass cells using purified water as reference. Absorbance spectra were obtained for the 400-750 nm range at 1-nm intervals. With all samples, the optical density at 700 nm was low (0.0000±0.0001), and for uniformity, it was null-point corrected at this wavelength[27]. The absorption coefficient a (λ) was calculated from the corrected absorbance using the equation as follows:

$$a(\lambda) = 2.303\ A(\lambda)/0.1\ (m^{-1})$$

where 2.303 is ln(10) and 0.1 is the cuvette path length in meters. CDOM absorption decreases exponentially with increasing wavelength and can be modeled by an exponential decay curve:

$$a(\lambda) = a(\lambda_0)\ e^{-S(\lambda-\lambda o)}$$

where a = Napierian absorption coefficient (m^{-1}), a(λ) is the absorption coefficient at wavelength λ (nm), λ_0 is a reference wavelength (nm), and *S* is referred to as spectral slope. CDOM concentration is expressed as absorption coefficient [$a_{CDOM}(440)$][18]. The spectral slope, S, was calculated by fitting an exponential regression model to the absorption coefficient versus wavelength (see the above equation).

Spectral slopes provide further insights into the average characteristics (size, source) of CDOM than absorption value alone, S are independent of CDOM concentration[28]. S has been used for correcting remote sensing (bio-optics) data[29] and monitoring CDOM degradative processes[30]. S also used to semi quantitatively describes the ratio of fulvic acids (FA) to humic acids (HA) in a sample[31]. Similarly it was noted that S correlates strongly with molecular weight (MW) of isolates of fulvic acids but not humic acids [31, 32].

Statistical Analysis

All physico-chemical data were expressed in terms of mean ± SD (standard deviation). The Pearson correlation coefficient (*r*) was also computed between the $a_{CDOM}(440)$ and corresponding physico-chemical parameters along with chl-*a*.

Results and Discussion

Physico-chemical conditions during the study period

The present study has been conducted from October, 2014 to March, 2015. Among these six months, November to February marks the winter season, while October and March are prior and post month of winter season, respectively. SST was quite high in October (30.4 ± 0.4 °C), and it gradually decreased until January due to the prevalence of winter in this region (Table 1). However, from February onwards, it again showed an increasing trend. SSS showed an opposite trend compared to SST as it increased from October to January. In October it was lowest (19.9 ± 0.5 ppt) as the effect of monsoon freshwater discharge was still in vogue, however, with the advent of winter months the river flow became diminished and the SSS increased. In February and March a marginal decrease was observed. Like SSS, TSM is also found to be principally regulated by the freshwater flow in this area. In October, when the effect of monsoon was prominent, the TSM was as high as 46.9 ± 1.6 mg l^{-1}, while in February, i.e. in the lean period it decreased up to 23.4 ± 1.5 mg l^{-1}. Chl-*a* (as a proxy of phytoplankton) did not exhibit any such temporal trend, however, during the month of January, the surface chl-*a* concentration increased than October. In February also it was quite high. Biswas et al. (2010)[22] also observed similar higher concentrations of chl-*a* during this time of the year near the Mouth of River Hugli. DO was under-saturated throughout the study period, however, it was found maximum in February (6.4 ± 0.2 mg l^{-1}), and while in November it was observed to be the lowest (4.6 ± 0.4 mg l^{-1}). The main source of nutrients in this coastal waters are driven by the discharge of Hugli Estuary, hence their concentration has decreased steadily from October with decreased run off in (Table 1) the winter months. Similar trends of physico-chemical parameter and nutrient variability were observed in a four year long study in the very same region[33].

Variability of $a_{CDOM}(440)$ during the study period

The $a_{CDOM}(440)$ varied between 0.1110 m^{-1} and 0.1422 m^{-1} during the winter. The maximum value (i.e. 0.2411 m^{-1}) was observed during the month of October, when the effect of monsoon driven freshwater flow and River Hugli discharge were more active. In the northwestern Bay of Bengal, Pandi et al (2013)[34] described the range of $a_{CDOM}(440)$ (i.e. 0.120 - 0.252 m^{-1}), while working during monsoonal period. Chiranjeevulu et al (2014)[35] reported $a_{CDOM}(350)$ range 0.322 – 5.067 m^{-1} (monsoon) and 0.368 – 1.934 m^{-1} (premonsoon) working on the Indian central east coast in the Bay of Bengal. Furthermore, In the coastal Yellow Sea and East China Sea, the observed range of the absorption coefficient of CDOM is 0.67 – 0.08 m^{-1} [36]. The minimum value was observed during March (i.e. 0.0862 m^{-1}) after winter in this study region. On the whole the average $a_{CDOM}(440)$ gradually decreased from October onwards. This might be due to the fact that most of the materials responsible for the increased absorbance of CDOM are principally governed by the freshwater flow of the Hugli Estuary and water flushing of the mangrove forest. Hence as the effect of monsoon faded and lean period advanced the $a_{CDOM}(440)$ slowly decreased (Fig 2), though slim high value observed during end of January.

Table 1─Monthly mean (±standard deviation) of physico-chemical parameters and nutrients of the study region

	Oct,14	Nov,14	Dec,14	Jan,15	Feb,15	March, 15
SST	30.4 ± 0.4	26.2 ± 0.3	23.5 ± 0.3	21.6 ± 0.2	22.1 ± 0.2	23.5 ± 0.4
SSS	19.9 ± 0.5	22.8 ± 0.6	26.9 ± 0.5	29.8 ± 0.3	28.4 ± 0.1	26.4 ± 0.2
TSM	46.9 ± 1.6	37.6 ± 3.5	22.3 ± 5.1	27.7 ± 2.6	23.4 ± 1.5	29.8 ± 3.4
Chl-*a*	0.35 ± 0.05	0.29 ± 0.04	0.32 ± 0.07	1.43 ± 0.05	0.93 ± 0.40	0.56 ± 0.08
D.O.	4.8 ± 0.7	4.6 ± 0.4	4.7 ± 0.2	4.9 ± 0.1	6.4 ± 0.2	5.2 ± 0.1
DIN	10.11 ± 0.52	9.65 ± 0.11	6.15 ± 0.22	4.12 ± 0.25	2.71 ± 0.27	2.35 ± 0.12
DIP	2.11 ± 0.22	0.71 ± 0.11	0.61 ± 0.07	0.65 ± 0.05	0.5 ± 0.12	0.62 ± 0.05
Silicate	11.22 ± 0.49	10.21 ± 1.11	7.02 ± 0.07	5.61 ± 0.17	5.01 ± 0.03	3.98 ± 0.17

Unit: SST (°C), SSS (ppt), TSM (mg l^{-1}), Chl-*a* (mg m^{-3}), D.O. (mg l^{-1}), DIN (µM), DIP (µM) and Silicate (µM). (n = 6, for all the parameters in each month)

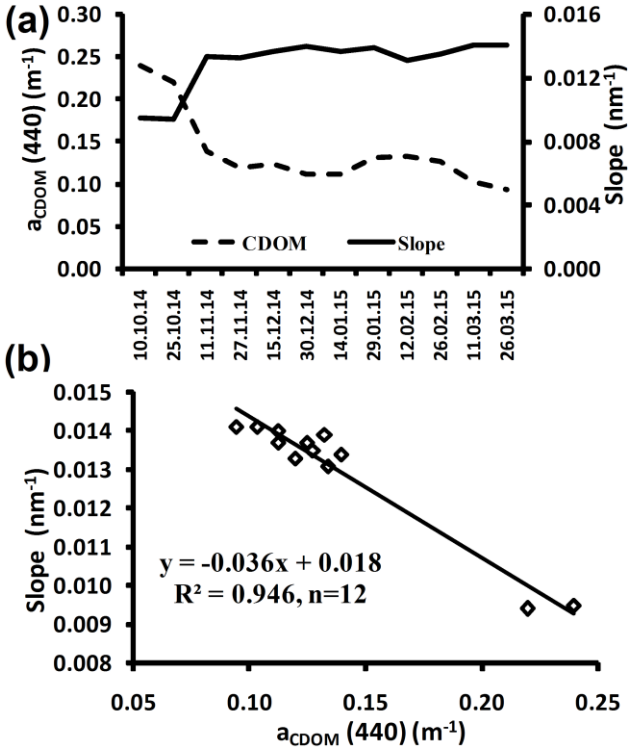

Fig. 2─Relationship between $a_{CDOM}(440)$ and Slope (400-700) a. Line graph b. Scatter graph

Spectral Slope Character of CDOM

The spectral slope values, S, were in the range of 0.0095-0.0141 nm^{-1} and fit to a significant inverse linear model with $a_{CDOM}(440)$ (Fig. 2):
$S = - 0.036\ a_{CDOM}(440) + 0.018$ ($R^2 = 0.946$, N = 12, p = 0.0001). The mean slope of the conservative $a_{CDOM}(440)$ in the winter season was 0.0138±0.0021 nm^{-1}, close to the global average of 0.014 nm^{-1} [37]. Pandi et al. (2013)[34] reported mean slope (i.e. 0.0143±0.0021 nm^{-1}) working on the northwestern Bay of Bengal which having river influence. The slope value can be used as proxy of DOM size [34]. This study region is significantly affected by the discharge of Hugli and other rivers. Prior of winter (October), the slope was low (Fig.2) and the CDOM molecular weight was high, when dilution effect was more in the study region because of monsoon. Slope increased (Fig 2) as well CDOM molecular weight has decreased from November with decreasing run off in the winter season.

Correlation of $a_{CDOM}(440)$ with relevant parameters

The observations discussed in the previous section indicate that CDOM absorbance in this study area has a monthly variation and it might be significantly governed by the freshwater inputs. Moreover, Chl-*a* has the potential of regulating the availability of CDOM in natural waters[38]. In order to quantify their effects and develop an idea about the behavior of CDOM with respect to these phenomenon, a correlation coefficient matrix is prepared between $a_{CDOM}(440)$ and those parameters which can logically have an influence over CDOM (Table 2). Since the present study has been carried out at a fixed point in these coastal waters over consecutive months, SSS and TSM can be considered as a proxy of the fresh - ocean water mixing. Chl-*a* along with SST values were also correlated.

Table 2─The Pearson correlation coefficient matrix between CDOM, TSM, SSS, SST and Chl-*a*

		CDOM	SSS	Chla	TSM
SSS	r	-0.763**			
	p	0.000			
Chl-*a*	r	-0.242	0.669**		
	p	0.154	0.000		
TSM	r	0.765**	-0.886**	-0.384*	
	p	0.000	0.000	0.021	
SST	r	0.833**	-0.981**	-0.601**	0.875**
	p	0.000	0.000	0.000	0.000

**p< 0.01, i.e. correlation is significant at the 0.01 level.

The observations discussed in the previous section indicate that CDOM absorbance in this study area has a monthly variation and it might be significantly governed by the freshwater inputs. Moreover, Chl-*a* has the potential of regulating the availability of CDOM in natural waters[38]. In order to quantify their effects and develop an idea about the behavior of CDOM with respect to these phenomenon, a correlation coefficient matrix is prepared between $a_{CDOM}(440)$ and those parameters which can logically have an influence over CDOM (Table 2). Since the present study has been carried out at a fixed point in these coastal waters over consecutive months, SSS and TSM can be considered as a proxy of the fresh - ocean water mixing. Chl-*a* along with SST values were also correlated.

The $a_{CDOM}(440)$ values observed are similar like other several coastal regions[39,40,19,38,41,42]. The significant inverse linear relationship of $a_{CDOM}(440)$ with salinity (Fig.3b): $a_{CDOM}(440) = - 0.011 \times \text{Salinity} + 0.444$ ($R^2 = 0.801$, N=26, $p<0.001$) indicates to the conservative mixing of marine and terrestrial end members to control $a_{CDOM}(440)$ largely. Pandi et al. 2013[34] also reported a significant inverse linear

relationship between $a_{CDOM}(440)$ and salinity, i.e. $a_{CDOM}(440) = - 0.011 \times \text{Salinity} + 0.429$ ($R^2 = 0.77$). Several other studies also reported the same trend of correlation between $a_{CDOM}(440)$ and salinity[43, 44, 45, 46]. The $a_{CDOM}(440)$ was lower by 0.0862 m^{-1} when the calculated average salinity was ~ 30 ppt. This implies that as SSS increased throughout the winter due to reduced freshwater discharge, the $a_{CDOM}(440)$ decreased accordingly (Fig. 3). Similar to SSS, TSM also indicates the abundance of freshwater as the main source of TSM in this study area is driven by the perennial flow of the Hugli Estuary.

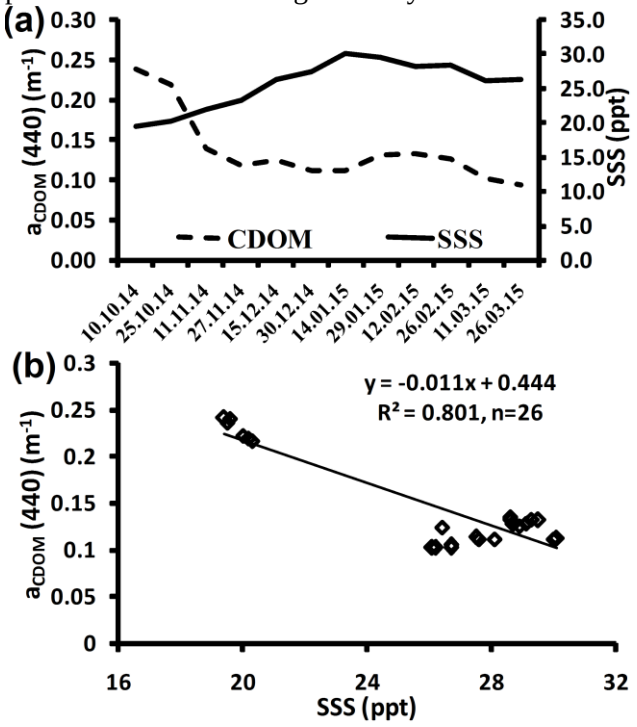

Fig. 3─Variation of $a_{CDOM}(440)$ with the sea surface salinity (SSS) during study period a. Line graph b. Scatter graph

As the lean period became strong the magnitude of TSM decreased and along with it the $a_{CDOM}(440)$ also decreased (Fig. 4). The strongest correlation (positive) was observed between $a_{CDOM}(440)$ and TSM out of all the parameters studied: $\text{TSM} = 157.4 \times a_{CDOM}(440) + 9.931$ ($R^2 = 0.779$, N=28, $p<0.001$). Correlation between both SSS and TSM with respect to $a_{CDOM}(440)$ clearly underlines the fact the CDOM variability in this study area is principally dominated by the freshwater flow and mangrove runoff.

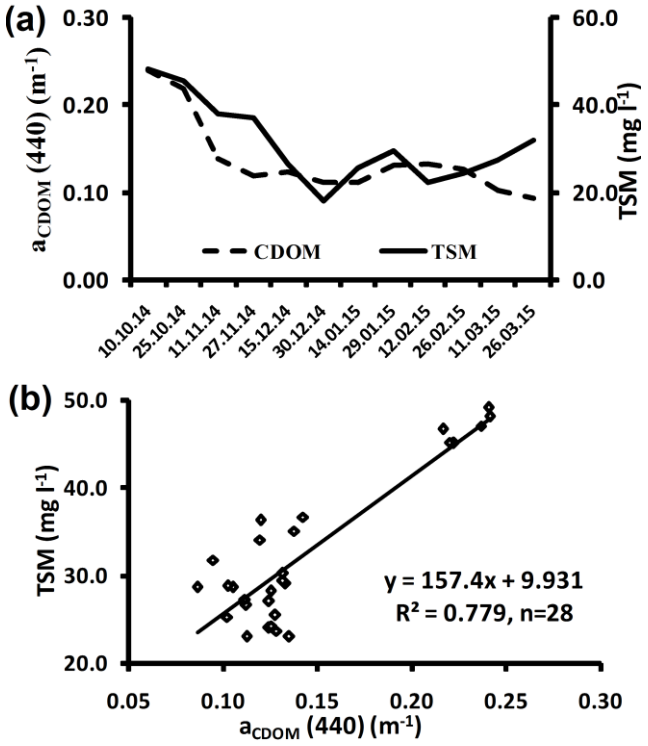

Fig. 4─Relationship between $a_{CDOM}(440)$ and TSM (Total suspended matter) during study time a. Line graph b. Scatter graph

No significant correlation between Chl-*a* and $a_{CDOM}(440)$ was observed (Fig. 5), Chl-*a* was quite low during October to December, however, during January and February, the chl-*a* values increased substantially. During this period a slight increase in $a_{CDOM}(440)$ was also observed (Fig. 5). Sasaki et al (2005)[38] also observed a significant increase of CDOM during and after a session of chl-*a* enhancement in Funka Bay, Hokkaido, Japan but found no correlation between CDOM and chl-*a*. Upon critically analyzing the cruise wise data of $a_{CDOM}(440)$ it can be seen that with the onset of winter the mean magnitude of $a_{CDOM}(440)$ almost halved from 0.2294 m^{-1} to 0.1249 m^{-1}. Until the end of winter, the value of $a_{CDOM}(440)$ remained approximately constant, however, just after the chl-*a* value was highest the $a_{CDOM}(440)$ values increased to around 0.1320 m^{-1} again. This shows that the initial peak could be attributed to higher freshwater flow, while the second mild peak might be due to phytoplankton debris. Since CDOM is nothing but a fraction of DOM its abundance was also affected by this mean.

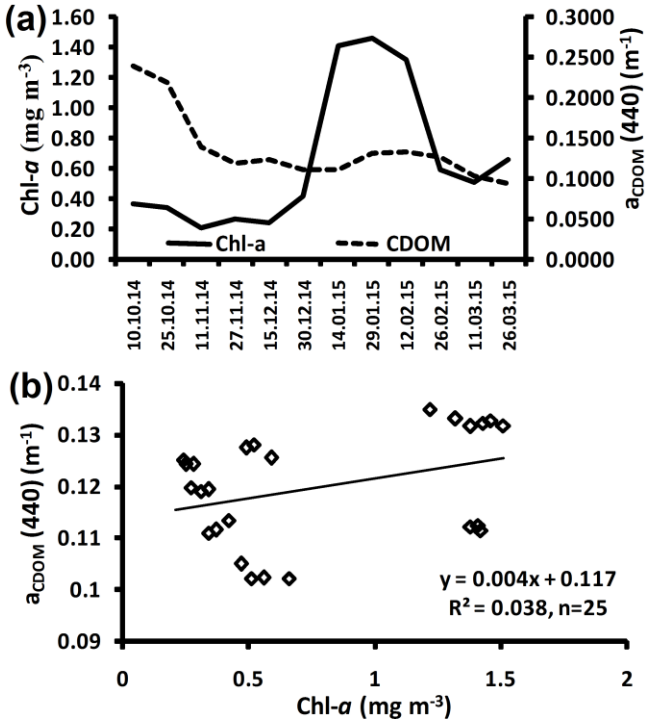

Fig. 5─Correlation plot of $a_{CDOM}(440)$ with the average chlorophyll-*a* concentration a. Line graph b. Scatter graph

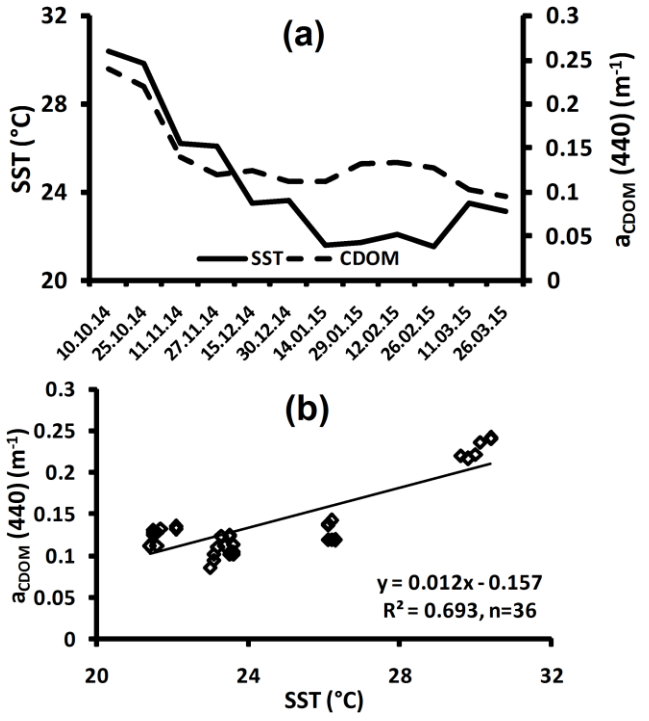

Fig. 6─Correlation plot of $a_{CDOM}(440)$ with the average sea surface temperature (SST) a. Line graph b. Scatter graph

A positive correlation between SST and $a_{CDOM}(440)$ was also observed (Table 2; Fig. 6), i.e. $a_{CDOM}(440) = 0.012 \times SST - 0.157$ ($R^2 = 0.693$, n= 36); however, this correlation might be spurious as the variation of temperature coincided with other logical parameters like SSS and TSM. However, it would be erroneous to establish relationship between them from this kind of short term regional study. Moreover, Fig. 7 has shown the Shimadzu UV-Visible 1600 double-beam spectrophotometer generated wavelength vs absorbance spectral graph of the coastal water. UV-Visible absorption spectra for CDOM increase exponentially with decreasing wavelength; this was also observed by other researchers in the past[18].

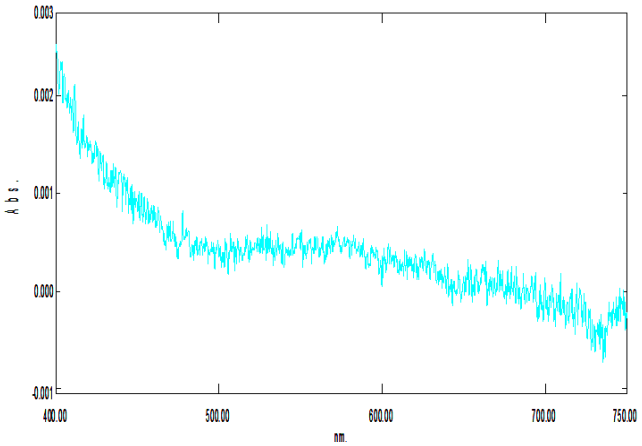

Fig. 7─UV-Visible Spectrophotometer generated CDOM absorption curve (Absorbance vs Wave length) sampling on 30th December, 2014

Conclusion

Distinct optical and hydro-chemical conditions have been observed in the nBoB coastal water lying adjacent to West Bengal coast, in effect of river discharge and other factors. The measurements conducted in the present study can lead us to infer that $a_{CDOM}(440)$ had a substantial monthly variability during the study time. In this study region, CDOM characteristics namely $a_{CDOM}(440)$ and S are principally controlled by variability of freshwater discharge from River Hugli and monsoonal runoff through mangrove ecosystem of Sundarban. Mild increasing trend of the $a_{CDOM}(440)$ was also observed during the months of January and February. A preliminary, first observation about the range and magnitude of CDOM was accomplished by means of this study in the shallow coastal water of northern part

of Bay of Bengal adjacent to West Bengal during the study period. CDOM concentration [$a_{CDOM}(440)$] and composition (slope) are distinctly different in the month of October compared to winter period. Correction factors for a_{ph}, a_D and phytoplankton community structure should be incorporated to evaluate correct chl-*a* algorithm of this coastal sea in future.

Acknowledgement

The study was funded by Indian National Centre for Ocean Information Services (INCOIS) (INCOIS: F&A: XII: A1:031), Ministry of Earth Sciences, India under Marine Fisheries Advisory Services (MFAS) programme. The authors are thankful to the Director of INCOIS for encouragement.

References

1 Branco, A. B. & Kremer, J. N., The relative importance of Chlorophyll and Colored Dissolved Organic Matter (CDOM) to the Prediction of the Diffuse Attenuation Coefficient in Shallow Estuaries. *Estuaries*, 28(5) (2005), 643-652.

2. Prieur, L. & Sathyendranath, S., An optical classification of coastal and oceanic waters based on the specific spectral absorption curves of phytoplankton pigments, dissolved organic matter, and other particulate materials, *Limnol. Oceanogr*., 26(4) (1981), 671-689.

3. Carder, K. L., Hawes, S. K., Baker, K. A., Smith, R. C., Steward, R. G. & Mitchell, B. G., Reflectance model for quantifying chlorophyll-*a* in the presence of productivity degradation products, *J. Geophys. Res*., 96(C11) (1991), 20599– 20611.

4. Mobley, C. D., *Light and Water*: Radiative transfer in natural waters, (Academic Press, San Diego, California) 2001, pp.2321-2330.

5. Siegel, D. A., Maritorena, S., Nelson, N. B., Behrenfeld, M. J. & McClain, C. R., Colored dissolved organic matter and its influence on the satellite-based charaterization of the ocean biosphere, *Geophys. Res. Lett.*, 32(L20605) (2005), doi:10.1029/2005GL024310.

6. Benner R, Chemical composition and reactivity, in: *Biogeochemistry of marine dissolve organic matter*, edited by D. A. Hansell & C. A. Carlson, (Academic Press, San Diego, California) 2002, pp. 59-90.

7. Blough N V & Del Vecchio, Chromophoric DOM in the coastal environment, in: *Biogeochemistry of marine dissolved organic matter*, edited by D. A. Hansell & C A Carlson, (Academic Press, San Diego, California) 2002, pp. 509-546.

8. Coble, P. G., Marine optical biogeochemistry: the chemistry of ocean color, *Chem Rev*, 107 (2007) 402-418, doi: 10.1021/cr050350+.

9. Twardowski, M. S. & Donaghay, P. L., Photobleaching of aquatic dissolved materials: absorption removal, spectral alteration, and their interrelationship, *J Geophys Res*, 107(C8) (2002) 6.1-6.12.

10. Chang, G. C. & Dickey, T. D., Coastal ocean optical influences on solar transmission and radiant heating rate, *J.Geophys.Res.*, 109 (2004) C01020, doi:10.1029/2003JC001821.

11. Dierssen, H. M., Perspectives on empirical approaches for ocean color remote sensing of chlorophyll in a changing climate, *PNAS*, 107(2010), 17073-17078.

12. Kalle, K., The problem of Gelbstoff in the sea, *Oceanogr Mar Biol Annu*, 4(1966), 91-104.

13. Jerlov N G, *Optical Oceanography*, (Elsevier, New York) 1968, pp.194.

14. Bricaud, A., Morel, A. & Prieur, L., Absorption by dissolved organic matter of the sea (yellow substance) in the UV and visible domains, *Limnol Oceanogr*, 28(1981), 43-53.

15. Siegel, D. A., Maritorena, S., Nelson, N. B., Hansell, D. A. & Lorenzi-Kayser, M., Global distribution and dynamics of colored dissolved and detrital organic materials, *J Geoohys Res.* , 107(C3228)(2002), doi: 10.1029/2001JC000965.

16. Nelson, N. B., Siegel, D. A., Carlson, C. A., Swan, C., Smethie, W. M. & Khatiwala, S., Hydrography of chromophoric dissolved organic matter in the North Atlantic, Deep-Sea Res I, 54(2007), 710-731.

17. Dong, Q., Shang, S. & Lee, Z., An algorithm to retrieve absorption coefficient of chromophoric dissolved organic matter from ocean color, *Remote Sens Environ*, 128(2013), 259-267.

18. Twardowski, M. S., Boss, E., Sullivan, J. M. & Donaghay, P. L., Modelling the spectral shape of absorbing chromophoric dissolved organic matter, *Mar Chem*, 89(2004), 69-88.

19. Stedmon, C. A. & Markager, S., Behaviour of the optical properties of coloured dissolved organic matter under conservative mixing, *Estuarine, Coastal and Shelf Science*, 57(2003), 01-07.

20. Varkey M J, Murty V S N & Suryanarayana A, Physical oceanography of the Bay of Bengal and Andamann Sea; in: *Oceanography and Marine Biology*, edited by A. D. Ansell, R. N. Gibson and M. Barnes (UCL, London) 34 1996, pp. 1-70.

21. Unger, D., Ittekkot, V., Schafer, P., Tiemann, J. & Reschke, S., Seasonality and interannual variability of particle fluxes to the deep Bay of Bengal: Influence of riverine input and oceanographic processes, *Deep-Sea Res. II*, 50(2003), 897–923.

22. Biswas, H., Dey, M., Ganguly, D., De, T. K., Ghosh, S. & Jana, T. K., Comparative Analysis of Phytoplankton Composition and Abundance over a Two-Decade Period at the Land–Ocean Boundary of a Tropical Mangrove Ecosystem, *Estuar Coast*, 33(2010), 384–394.

23. Gomes, H. R., Goes, J. I. & Saino, T., Influence of physical processes and freshwater discharge on the seasonality of phytoplankton regime in the Bay of Bengal, *Continen. Shelf. Res.*, 20(2000), 313–330.

24. Madhupratap, M. M., Gauns, M., Ramaiah, N., Kumar, S. P., Muraleedharan, P. M., Sousa, S. N., Sardessai, S. & Muraleedharan, M., Biogeochemistry of the Bay of Bengal: physical, chemical and primary productivity characteristics of the central and western Bay of Bengal during summer monsoon 2001, *Deep-Sea Res. II***,** 50(2003), 881–896.

25. APHA, 2005, Standard methods for examination of water and wastewater, 21st edn. American Public Health Association, American Water Works Association, Water Pollution Control Federation, New York.

26. Carritt, D. E. & Carpenter, J. H., Comparison and evaluation of currently employed modification of Winkler method for determination of dissolved oxygen in seawater, A NASCO Report, *J Mar Res*, 24(1966), 287-318.

27. Shank, C. G., Nelson, K. & Montagna, K., Importance of CDOM distribution and photo reactivity in a shallow Texas

Estuary, *Estur Coasts*, 32(2009), 661-677.
28. Brown, M., Transmission spectroscopy examinations of natural waters, *Estuar Coast Mar Sci*, 5(1977), 309-317.
29. Schwarz, J. N. & others, Two models for absorption by coloured dissolved organic matter (CDOM), *Oceanologia*, 44(2002), 209-241.
30. Vahatalo, A. V. & Wetzel, R. G., Photochemical and microbial decomposition of chromophoric dissolved organic matter during long (months-years) exposures, *Mar Chem*, 89(2004), 313-326.
31. Carder, K. L., Steward, R. G., Harvey, G. R. & Ortner, P. B., Marine humic and fulvic acids: Their effects on remote sensing of ocean chlorophyll, *Limnol Oceanogr*, 34(1989), 68-81.
32. Hayase, K. & Tsubota, H., Sedimentary humic-acid and fulvic-acid as fluorescent organic materials, *Geochim Cosmochim Acta*, 49(1985), 159-163.
33. Das, S., Chanda, A., Giri, S., Akhand, A. & Hazra, S., Characterizing the influence of tide on the physico-chemical parameters and nutrient variability in the coastal surface water of northern Bay of Bengal (nBoB) during winter season, *Acta Oceanol Sinica*, 34(12) (2015), 102-111.
34. Pandi, S. R., Kiran, R., Sarma, N. S., Srikanth, A. S., Sarma, V. V. S. S., Krishna, M. S., Bandyopadhyay, D., Prasad, V. R., Acharyya, T. & Reddy, K. G., Contrasting phytoplankton community structure and associated light absorption characteristics of the western Bay of Bengal, *Ocean. Dynam.*, (2013), doi 10.1007/s10236-013-0678-1.
35. Chiranjeevulu, G. K., Murty, K. N., Sarma, N. S., Kiran, R., Chari, N. V. H. K., Pandi, S. R., Venkatesh, P., Annapurna, C. & Rao, K. N., Colored dissolved organic matter signature and phytoplankton response in a coastal ecosystem during mesoscale cyclonic (cold core) eddy, 2014, *Mar. Environ. Res.*, (2014), 1-11.
36. Huang, J., Chen, L., Chen, X. & Song, Q., Validation of semi-analytical inversion models for inherent optical properties from ocean color in coastal Yellow Sea and East China Sea, *J. Oceanogr.*, 69(2013), 713–725.
37. Del, Castillo. C. E. & Coble, P. G., Seasonal variability of the colored dissolved organic matter during the 1994-1995 NE and SW Monsoons in the Arabian Sea, *Deep-Sea Rea II*, 47(2000), 1563-1579.
38. Sasaki, H., Miyamura, T., Saitoh, S. & Ishizaka, J., Seasonal variation of absorption by particles and colored dissolved organic matter (CDOM) in Funka Bay, southwestern Hokkaido, Japan, *Estuar. Coast. Shelf Sci*, 64(2005), 447-458.
39. Davis-Colley, R. J., Yellow substance in coastal and marine waters round the South Island, New Zealand, *J. Mar. Freshwat. Res.*, 26(1992), 311-322.
40. Stedmon, C. & Markager, S., The optics of chromophoric dissolved organic matter (CDOM) in the Greenland Sea: an algorithm for differentiation between marine and terrestrially derived organic matter, *Limnol Oceanogr*, 46(2001), 2087-2093.
41. Loisel, H., Meriaux, X., Poteau, A., Artigas, L. F., Lubac, B., Gardel, A., Caillaud, J. & Lesourd, S., Analyze of the inherent optical properties of French Guiana coastal waters for remote sensing applications, *J. Coast. Res.*, 56(2009), 1532-1536.
42. Bowers, D., Md-Suffian, I. & Mitchelson-Jacob, E. G., Bio-optical properties of east coast Malaysia waters in relation to remote sensing of chlorophyll, *Int J Remote Sens*, 33(2012), 150-169.
43. Belanger, S., Xie, H., Krotkov, N., Larouche, P., Vincent, W. F. & Babin, M, Photomineralization of terrigenous dissolved organic matter in Arctic coastal waters from 1979 to 2003: Interannual variability and implications of climate change, *Global Biogeochem. Cycles*, 20(2006), doi:10.1029/2006GB002708.
44. Nieke, B., Reuter, R., Heuermann, R., Wang, H., Babin, M. & Therriault, J. C., Light absorption and fluorescence properties of chromophoric dissolved organic matter (CDOM), in the St. Lawrence Estuary (Case 2 waters), *Cont. Shelf Res*., 17(1997), 235– 252.
45. Matsuoka, A., Bricaud, A., Benner, R., Para, J., Sempere, R., Prieur, L., Belanger, S. & Babin, M., Tracing the transport of colored dissolved organic matter in water masses of the Southern Beaufort Sea: relationship with hydrographic characteristics, *Biogeosciences*, 9(2012), 925–940 doi:10.5194/bg-9-925-2012.
46. Branco, A. B. & Kremer, J. N., The Relative importance of chlorophyll and colored dissolved organic matter (CDOM) to the prediction of the diffuse attenuation coefficient in shallow estuaries, *Estuaries*, 28(5) (2005), 643 652.